# Adaptive optics performance over long horizontal paths: aperture effects in multi-conjugate adaptive optical systems

**Miao Yu**
*Department of Mechanical Engineering and Institute for Systems Research, University of Maryland*
**Mikhail A. Vorontsov**
*Intelligent Optics Laboratory, Computational and Information Sciences Directorate, U.S. Army Research Laboratory, and Intelligent Optics Laboratory, Institute for Systems Research, University of Maryland*
**Svetlana L. Lachinova**
*Intelligent Optics Laboratory, Institute for Systems Research, University of Maryland*
**Jim F. Riker**
*AFRL/DESM, Air Force Research Laboratory*
**V. S. Rao Gudimetla**
*AFRL/DESM, Air Force Research Laboratory*

## ABSTRACT

We analyze various scenarios of the aperture effects in adaptive optical receiver-type systems when inhomogeneities of the wave propagation medium are distributed over long horizontal propagation path, or localized in a few thin layers remotely located from the receiver telescope pupil. Phase aberration compensation is performed using closed-loop control architectures based on phase conjugation and decoupled stochastic parallel gradient descent (D-SPGD) control algorithms. Both receiver system aperture diffraction effects and the impact of wavefront corrector position on phase aberration compensation efficiency are analyzed for adaptive systems with single or multiple wavefront correctors.

## 1. INTRODUCTION

The primary idea of adaptive phase distortion correction is based on the assumption that the influence of optical inhomogeneities along the optical wave propagation path can be accounted for by using an "equivalent" thin phase-distorting layer (phase screen) located at the receiver telescope pupil-plane (pupil-plane phase screen) [1-4]. Although this assumption is adequate for many systems, the limitations of the pupil-plane phase screen model are found to affect a number of applications, especially for light beam propagation over nearly long horizontal propagation paths. These limitations result in intensity fluctuations (scintillations) at the receiver telescope pupil-plane that are typically accompanied by the appearance of singularities in the wavefront phase known as branch points or phase dislocations [5-8]. These effects are a result of optical wave propagation (diffraction) through a medium with spatially distributed or layered refractive index inhomogeneities.

Wavefront phase sensing and reconstruction under conditions of strong intensity scintillations have been extensively studied with emphasis on the development of wavefront sensing and control techniques that are robust to intensity scintillations [9-10]. As a well-known compensation strategy evoke from the pupil-plane phase screen model, phase conjugation compensation faces great difficulty in the presence of distant phase-distorting layers. The legitimacy of the phase conjugation compensation rule for the case of distant phase perturbations can be formally preserved in the approach known as multi-conjugate adaptive optics (MCAO) [9-15]. The MCAO technique is based on the use of several wavefront phase correctors placed in the image planes of the corresponding phase-distorting layers (conjugate planes). The phase conjugation correction is applied at each of the conjugated planes in the right sequence (from the pupil-plane toward the most remotely located layer).

There are several alternatives to the phase conjugation control strategy for use in compensating phase distortions due to distant phase-distorting layers. Among these approaches are adaptive control techniques based on direct

optimization of receiver system performance metrics [16-20]. The selected performance metrics, such as the Strehl ratio *St* or power-in-the-bucket (PIB), are dependent on the far-field intensity distribution of the corrected wave and can be referred to as far-field metrics.

Far-field metric optimization can be achieved using various gradient descent techniques or global optimization methods. The major problem with the far-field metric optimization technique is its relatively slow convergence rate. A significant improvement in the convergence rate can be achieved with the recently introduced adaptive optics technique referred to as decoupled stochastic parallel gradient descent (D-SPGD) [21]. D-SPGD adaptive wavefront control is robust with respect to intensity scintillations and can provide a rapid convergence rate even for high-resolution compensations [22].

In this paper, we consider both the traditional adaptive optics technique and an alternative model-free control strategy [e.g., wavefront control based on a decoupled stochastic gradient descent (D-SPGD) technique]. Both receiver system aperture diffraction effects and the impact of wavefront corrector position on phase aberration compensation efficiency are analyzed in various adaptive receiver scenarios. The rest of the article is organized as follows. In Section 2, the system architecture of the adaptive receiver system is described. In Section 3, numerical model and various parameters are introduced. In Section 4, the aperture effects on the adaptive receiver system performance are discussed. The concluding remarks are made in the Section 5.

## 2. ADAPTIVE RECEIVER SYSTEM FOR COMPENSATION OF LASER BEAM PROPAGATION OVER LONG HORIZONTAL PATH

### 2.1 System Schematic

A schematic of the adaptive receiver system is shown in Fig. 1. This system consists of the following major components: (a) a wave propagation path with a set of thin, random phase-distorting layers [phase-screens $\varphi_j(\mathbf{r})$,

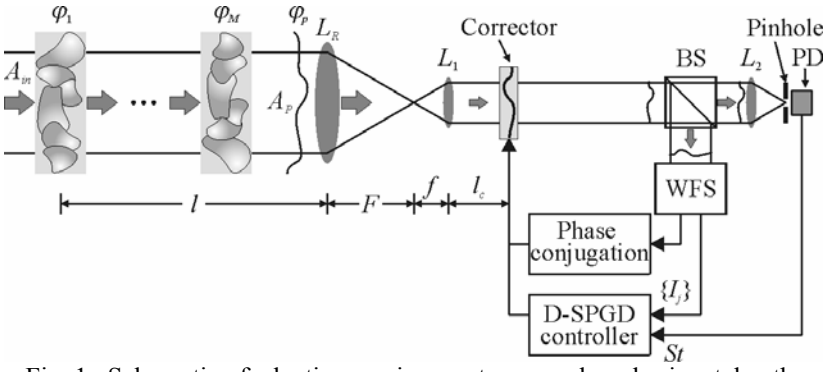


Fig. 1. Schematic of adaptive receiver system over long horizontal path.

$j = 1, \ldots, M$] equally spaced over the propagation distance $l$; (b) a receiver telescope (lens $L_R$) and lens $L_1$ confocal to lens $L_R$; (c) a wavefront corrector located a distance $l_c$ from the lens $L_1$; (d) a near-field wavefront sensor (WFS); (e) a far-field sensor (lens $L_2$ and a pinhole with photo-detector located behind it); and (f) a phase conjugation and a D-SPGD controller supplying (in a sequence) to the corrector actuators the control signals $\{u_j\}$ (where $j = 1, \ldots, N$), or the control signals that include small perturbations $\{\delta u_j\}$.

For simplicity, assume that the lens system $L_R$ and $L_1$ have the same focal length ($F = f$). To simplify notation, we omit time dependency by assuming that optical inhomogeneities along the propagation path are fixed ("frozen"). In general, a wavefront corrector can be positioned at any plane if its size matches the beam size in the optical receiver system wave-train. In this case, if we consider the wavefront corrector is placed in the conjugate plane of a phase screen located at position $l$, the wavefront corrector position can be easily determined to be $l_c = 2F - l$ from the lens $L_1$. For the case when wavefront corrector is placed at the conjugate plane of the pupil, $l_c = 2F$.

### 2.2 Wavefront Corrector

A rectangular array of $N = n_c \times n_c$ piston-type elements with zero spacing in between (100% fill factor) and the aperture size $D_c = n_c d_c$ is considered as the adaptive system wavefront corrector, where $d_c$ is the element size. The

phase modulation $u(\mathbf{r}) = \sum_{j=1}^{N} S_0(\mathbf{r} - \mathbf{r}_j)$ introduced by the corrector depends on the control signals (controls) $\{u_j\}$ and the stepwise influence functions $\{S_0(\mathbf{r} - \mathbf{r}_j)\}$ centered at the points $\{\mathbf{r}_j\}$ which coincide with the centers of the correcting elements. In most cases considered here, we assumed that the receiver telescope aperture, as well as the aperture of the re-imaging lens, match the corrector aperture, and hence $D_c$ can be regarded as the receiver aperture size.

### 2.3 Wavefront Sensors

The corrected wave with residual phase $\delta(\mathbf{r}) = u(\mathbf{r}) + \varphi(\mathbf{r})$ is divided by the beam splitter BS as shown in Fig. 1 with inputs to both the far-field and near-field wavefront sensors. The far-field wavefront sensor provides measurements of far-field metrics, which are proportional to the measures of optical system performance such as the Strehl ratio *St* and the power-in-the-bucket $P_b$. The Strehl ratio is given by the normalized on-axis focal plane intensity $I_F$: $St = I_F / I_F^0$, where $I_F^0$ is the on-axis intensity in the absence of phase aberrations. The power-in-the-bucket can be obtained from the integration of the focal plane intensity distribution $I_F(\mathbf{r})$ over a circular bucket area $\Omega_b = \pi b^2/4$, where $b$ is the diameter of a bucket, that is, $P_b = \int_{\Omega_b} I_F(\mathbf{r})\, \mathrm{d}^2\mathbf{r}$.

The near-field wavefront sensor can be based on the point-diffraction interferometer (PDI) [16, 23-24] or Shack-Hartmann wavefront sensor capable of accurate reconstruction of the phase function $\varphi(\mathbf{r})$. The near-field wavefront sensor transforms the residual wavefront phase aberration $\delta(\mathbf{r})$ in the distorted input field into the sensor output intensity $I_\delta(\mathbf{r})$, thus performing two-dimensional (2D) phase aberration sensing while the output signal of the far-field sensor measuring the far-field metrics (the Strehl ratio *St* and the power-in-the-bucket $P_b$) is a one-dimensional (1D) signal.

### 2.4 Phase Conjugation vs. D-SPGD Correction

Consider a phase conjugation controller with an ideal high-resolution wavefront sensor (e.g, Shack-Hartmann wavefront sensor) capable of accurate reconstruction of the pupil plane phase function $\varphi_p(\mathbf{r})$. The control signals $\{u_j\}$ in this case can be calculated using deconvolution of the reconstructed phase function $\varphi_p(\mathbf{r})$ over the wavefront corrector influence function. For the piston-type corrector, this corresponds to:

$$u_j = -\int_{\Omega_c} \varphi_p(\mathbf{r}) S_0(\mathbf{r} - \mathbf{r}_j)\, \mathrm{d}^2\mathbf{r} = -\int_{\Omega_j} \varphi_p(\mathbf{r})\, \mathrm{d}^2\mathbf{r}, \tag{1}$$

where $\Omega_c$ and $\{\Omega_j\}$ are the wavefront sensor/corrector aperture area and its sub-aperture regions, respectively. The control signals in the phase conjugation correction with a piston-type corrector can be computed by averaging the pupil-plane phase function $\varphi_p(\mathbf{r})$ over the sub-aperture areas $\{\Omega_j\}$.

In simulations of the phase conjugation correction, the phase function $\varphi_p(\mathbf{r})$ was reconstructed from the pupil-plane field complex amplitude $A_p(\mathbf{r})$ using the ratio of the imaginary $\mathrm{Im}[A_p(\mathbf{r})]$ part and the real $\mathrm{Re}[A_p(\mathbf{r})]$ part: $\varphi_p(\mathbf{r}) = \tan^{-1}\{\mathrm{Im}[A_p(\mathbf{r})]/\mathrm{Re}[A_p(\mathbf{r})]\}$. This corresponds to modeling of an ideal high-resolution wavefront sensor with a phase reconstructor. Because of the $2\pi$ periodicity of the function $\tan^{-1}$, the computed phase $\varphi_p(\mathbf{r})$ may contain $2\pi$ phase cuts (phase wraps) which were not removed prior to correction. At the points of the zero field $A_p(\mathbf{r}) = 0$, the phase $\varphi_p(\mathbf{r})$ can also contain branch points. In actual phase conjugation type systems, the phase $\varphi_p(\mathbf{r})$ is reconstructed from wavefront sensor data and may also contain $2\pi$ phase cuts and branch points. Removal of the $2\pi$ phase cuts and branch points is computationally expensive and is not done in most adaptive systems operating with piston-type correctors.

The D-SPGD controller performs an iterative update of the control voltages $\{u_j^{(n)}\}$. The $n$th step of the iteration process includes: (a) measurement of the near-field wavefront sensor output signals $\overline{I}_j^{(n)}$; (b) generation of the random (pseudo-random) perturbations $\{\delta u_j^{(n)}\}$ and computation of the perturbed control signals $\{u_j^{(n)} + \delta u_j^{(n)}\}$ applied to the corrector actuators (electrodes); (c) measurement of the sensor output signals $\{\overline{I}_j^{(n+1)}\}$ corresponding to the perturbed control parameters $\{u_j^{(n)} + \delta u_j^{(n)}\}$; (d) calculation of the sensor output perturbations

$\left\{\delta\overline{I}_j^{(n)}\right\} = \left\{\overline{I}_j^{(n+1)} - \overline{I}_j^{(n)}\right\}$; (e) computation of the products $\delta\overline{I}_j^{(n)}\delta u_j^{(n)}$; and (f) update of the controls in accordance with the following iterative procedure [21]:

$$u_j^{(n+1)} = u_j^{(n)} - \gamma^{(n)}\delta\overline{I}_j^{(n)}\delta u_j^{(n)}, \ (j = 1, \ldots, N), \tag{2}$$

where $\gamma^{(n)} > 0$ are the update or gain coefficients.

As shown in [21], iterative procedure (2) of the control signal update minimizes the near-field compensation performance metric:

$$J = \sum_{j=1}^{N}\overline{I}_j = \int\limits_{\Omega_c} I_\delta(\mathbf{r})\,\mathrm{d}^2\mathbf{r}\,. \tag{3}$$

The metric $J$ is proportional to the total light power at the wavefront sensor output.

## 3. NUMERICAL MODEL OF ADAPTIVE RECEIVER SYSTEM

### 3.1 Propagation Equation

Assume that a monochromatic and spatially coherent on-axis reference wave (beam) with optical field complex amplitude $A_{in}(\mathbf{r})$ propagates in an optically inhomogeneous medium (the atmosphere) toward an adaptive telescope receiver located a distance $z = l$ from the input plane $z = 0$ (plane of the farthest phase-distorting layer), as shown in Fig. 1. The complex amplitude of the input (reference) wave is given by:

$$A(\mathbf{r}, z = 0) = I_{in}^{1/2}(\mathbf{r})\exp\left[i\varphi_{in}(\mathbf{r})\right], \tag{4}$$

where $I_{in}(\mathbf{r})$ and $\varphi_{in}(\mathbf{r})$ are the intensity and phase distributions. Consider the input wave intensity distribution in the form:

$$I_{in}(\mathbf{r}) = I_0\exp\left[-\left(2|\mathbf{r}|^2/a_0^2\right)^n\right], \tag{5}$$

where $n = 8$ is chosen in the simulations, which corresponds to a super-Gaussian beam, and $a_0$ is the beam radius. We assume that the super-Gaussian beam has a diameter $2a_0$ exceeding the receiver telescope aperture diameter $D_c$.

### 3.2 Phase-Distorting Layers and Phase Perturbations Statistical Model

Assume that the refractive index inhomogeneties of the propagation medium can be modeled by a few relatively thin phase-distorting layers that principally contribute to the pupil-plane wavefront phase aberration $\varphi_p(\mathbf{r})$. For phase perturbations we consider realizations of the statistically homogeneous and isotropic random function $\varphi(\mathbf{r})$ with zero mean and Andrews power spectrum [25]:

$$G_A(q) = 2\pi 0.033\left(1.68/r_0\right)^{5/3}\left(q^2 + q_A^2\right)^{-11/6}\exp\left(-q^2/q_a^2\right)\left[1 + 1.802\left(q/q_a\right) - 0.254\left(q/q_a\right)^{7/6}\right]. \tag{6}$$

Here $r_0$ is the Fried parameter [26], and $q_A = 2\pi/l_{out}$ and $q_a = 2\pi/l_{in}$, where $l_{out}$ and $l_{in}$ are the outer and inner scales of the turbulence.

### 3.3 Numerical Model Parameters

The numerical grid size used in the computer simulations contained 512×512 pixels. The wavefront corrector (receiver aperture) size $D_c$ corresponds to the central grid area of 256×256 pixels. The phase perturbations $\varphi(\mathbf{r})$ were defined over the entire grid area (512×512 pixels). In the numerical simulations, the following normalized variables were used: $\hat{\mathbf{r}} = \mathbf{r}/a$, $\hat{l} = l/l_d$, and $\hat{l}_c = l_c/l_d$, where $l_d = 0.5ka^2$ is the diffractive length related to the beam radius $a = 2/3a_0$. The normalized by $l_d$ focal length $\hat{F}$ is fixed at $\hat{F} = 0.04$.

## 4. COMPENSATION EFFICIENCY OF ADAPTIVE OPTICAL SYSTEMS: APERTURE EFFECTS

### 4.1 Aperture Effects in Adaptive Optical System with Single Wavefront Corrector

Three models for propagation medium inhomogeneties are considered: (a) a single phase screen ($M = 1$) placed at the plane $z = 0$ [distant phase screen $\varphi_1(\mathbf{r})$], (b) two phase screens ($M = 2$) at the planes $z = l_1$ and $z = l_2$, and (c) a multi-layered phase-distorting medium model with $M = 10$ phase screens equally spaced over the distance $l$.

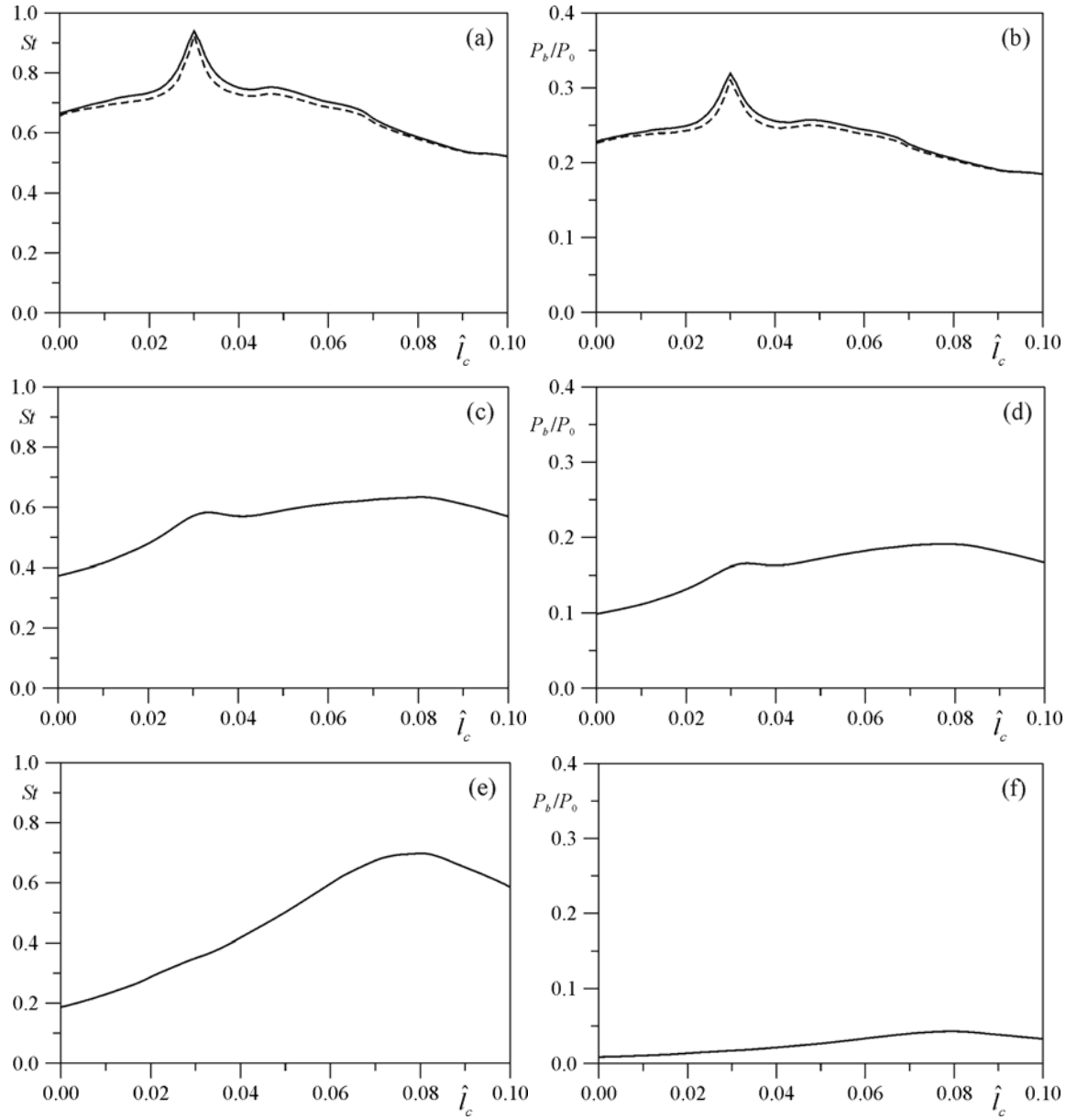


Fig. 2. Impact of single wavefront corrector position on phase aberration compensation efficiency for a single distant phase screen located a distance $\hat{l} = 0.05$ from the pupil-plane with $r_0 = 0.125$: ensemble-averaged Strehl ratio [(a), (c), (e)] and power-in-the-bucket [(b), (d), (f)] versus the normalized corrector distance for high-resolution phase-conjugated (solid curves) and D-SPGD (dashed curves) systems. (a), (b) represent the case for the receiver telescope with infinite aperture. (c), (d) represent the cases for the telescope having a finite aperture size of $D_c$ coincided with the corrector aperture and $D_c = 4/3a_0$. (e), (f) represent the cases for the telescope having a finite size aperture with $D_c = 2/3a_0$.

Consider the corrector displaced a distance $\hat{l}_c$ from the lens $L_1$, as shown in the system schematic in Fig. 1. The questions raised are: what is the impact of the corrector position on compensation efficiency? Where is the optimal position (distance $\hat{l}_c^{opt}$) for the wavefront corrector for single, or multiple distant phase-distorting layers?

For a single distant phase screen located a distance $\hat{l}$ from the telescope pupil, first, ignore aperture-induced diffraction effects by assuming an infinite aperture size for both the telescope $L_R$ and re-imaging lens $L_1$. The

dependence of the power-in-the-bucket $P_b$ and Strehl ratio <*St*> achieved after compensation process convergence on the normalized distance $\hat{l}_c = l_c / l_d$ is shown in Figs. 2(a) and 2(b) for both the high-resolution D-SPGD (dashed curve) and the phase-conjugated (solid curve) controllers. Note that compensation efficiency is estimated here by using the Strehl ratio <*St*> and the power-in-the-bucket $P_b$ calculated for the optical wave at the corrector plane after phase compensation was performed.

As expected, both the Strehl ratio dependence and the power-in-the-bucket dependence have a sharp peak (with a maximum value of <*St*> ≈1) at the distance $\hat{l}_c = 2\hat{F} - \hat{l} = 0.03$ ( $\hat{F} = 0.04$ , $\hat{l} = 0.05$ ), which corresponds to the conjugate plane of the phase screen. This indicates nearly perfect phase compensation and can only be achieved when aperture diffraction effects are neglected. Thus the optimal corrector position for both the phase conjugation and D-SPGD adaptive optical systems is in the plane conjugate to the distorting layer plane. Relocating the wavefront corrector from this plane causes the pure phase modulation to transform to intensity scintillations at the corrector, followed by a decrease in Strehl ratio and the power-in-the-bucket.

Next, consider compensation efficiency for a receiver telescope (lens $L_R$ in Fig. 1) with a finite aperture size of $D_c$. Assume that the telescope aperture coincides with the corrector aperture (after a corresponding scaling performed by the re-imaging lens $L_1$). The dependence of the ensemble-averaged Strehl ratio and the power-in-the-bucket on the normalized corrector displacement from the re-imaging lens $L_1$ for two different aperture sizes ($D_c = 4/3a_0$ and $D_c = 2/3a_0$) is shown in Figs. 2(c)–(f). As the aperture size decreases, the sharp peak corresponding to the corrector at the plane conjugate to the phase-distorting layer is smoothed out ($D_c = 4/3a_0$) and eventually disappears ($D_c = 4/3a_0$). Instead, the optimal wavefront corrector position shifts to the position at the conjugate pupil-plane ( $\hat{l}_c = 2\hat{F} = 0.08$ ).

The reason for such a change in optimal corrector position is telescope aperture-induced diffraction leading to parasitic intensity and phase modulation of the optical field in the corrector area, which is not present for an infinite telescope with perfect imaging of the distorting layer at the corrector area. This aperture-induced parasitic phase modulation cannot be distinguished from the phase perturbations introduced by the distorting layer, and hence adaptive compensation results in decrease in Strehl ratio and power-in-the-bucket. On the other hand, aperture diffraction effects do not impact the performance of a corrector positioned at the plane conjugate to the pupil-plane (assuming the re-imaging lens $L_1$ performs ideal imaging of the pupil-plane). In the presence of aperture diffraction effects, the optimal corrector position coincides with the conjugate pupil-plane.

Since Strehl ratio and power-in-the-bucket show similar behavior for the cases with infinite and finite receiver apertures, we only consider the adaptive receiver performance in terms of Strehl ratio in the following simulations.

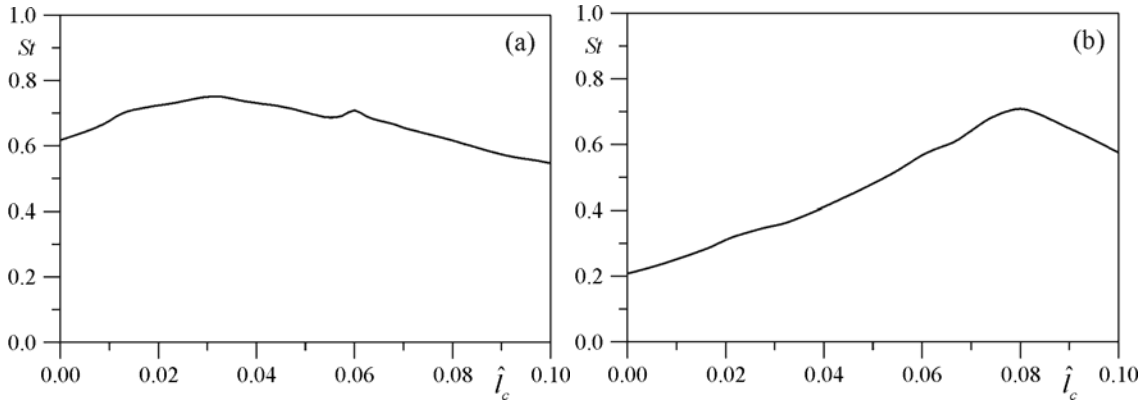


Fig. 3. Impact of single wavefront corrector position on phase aberration compensation efficiency for two phase screens spaced at the distances $\hat{l}_1 = 0.02$ and $\hat{l}_2 = 0.05$ : (a), (b) ensemble-averaged Strehl ratio versus the normalized wavefront corrector distance for high-resolution phase-conjugated control algorithms for the receiver telescope with infinite aperture (a), and for the telescope aperture coincided with the corrector aperture of size $D_c$ and $D_c = 2/3a_0$ (b).

Simulation results for two phase screens ($\hat{l}_1 = 0.02$ and $\hat{l}_2 = 0.05$) are presented in Fig. 3. For the infinite receiver aperture in Fig. 3(a) (no aperture diffraction), the optimal positions of the wavefront corrector (maximum Strehl ratio value) correspond to the distances $\hat{l}_{c1} = 0.06$ and $\hat{l}_{c2} = 0.03$, which are coincidence with the conjugate planes of the two phase screens. However, the peaks are not as sharp as the results obtained from one phase screen case [Fig. 2(a)]. In the presence of aperture diffraction effects ($D_c = 2/3a_0$), any advantage for positioning the wavefront corrector at the planes conjugate to the phase screens disappears [Fig. 3(b)]. The Strehl ratio curves in this case have a well-defined maximum corresponding to a corrector located at the conjugate plane of the telescope pupil.

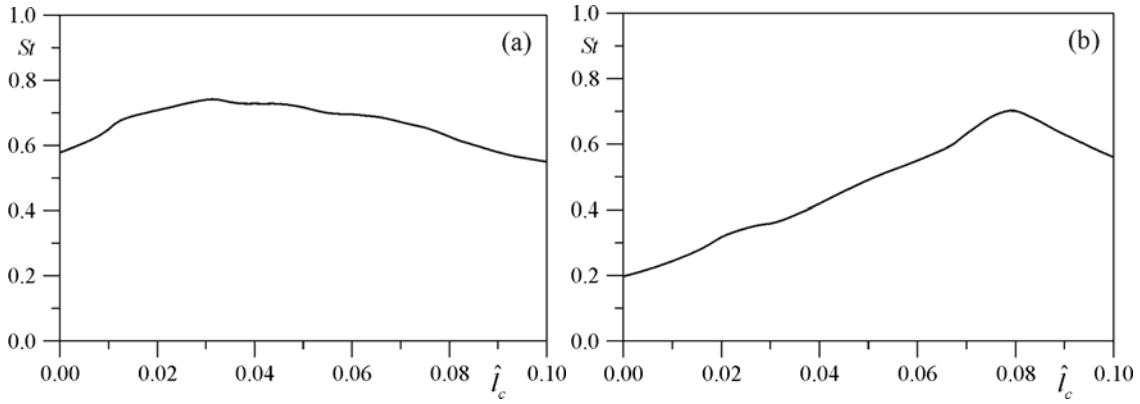


Fig. 4. Impact of single wavefront corrector position on phase aberration compensation efficiency for ten phase screens equally spaced over the distance $\hat{l} = 0.05$ : (a), (b) ensemble-averaged Strehl ratio versus the normalized wavefront corrector distance for high-resolution phase-conjugated control algorithms for the receiver telescope with infinite aperture (a), and for the telescope aperture coincided with the corrector aperture of size $D_c$ and $D_c = 2/3a_0$ (b).

Simulation results for multiple-distorting layers (ten phase screens equally spaced over the distance $l$) are presented in Fig. 4. For the infinite receiver aperture in Fig. 4(a) (no aperture diffraction), the optimal corrector position (maximum Strehl ratio value) at the distance $\hat{l}_c = 0.03$, which corresponds to the conjugate plane of the most remote located phase screen ($\hat{l} = 0.05$). The maximum value of the Strehl ratio curve in Fig. 4(a) exceeds the achieved Strehl ratio value for the corrector placed at the conjugate pupil-plane by less than 10%. Again, in the presence of aperture diffraction effects [Fig. 4(b)], the Strehl ratio curves have a maximum corresponding to a corrector located at the conjugate plane of the telescope pupil.

Because in most cases the geometry of the phase-distorting layers location is unknown or known with some degree of uncertainty, the results presented here suggest that there is no compelling reason for relocating the wavefront corrector from the conjugate plane of the telescope pupil, unless phase aberrations are the result of a single phase-distorting layer with an accurately defined location and aperture diffraction effects neglected.

### 4.2 Aperture Effects in Adaptive Optical System with Multiple Wavefront Correctors

Since MCAO techniques suggest that several wavefront phase correctors should be placed in the image planes of the corresponding phase-distorting layers (conjugate planes), it is also worthwhile to study the aperture effects in an adaptive optical system with multiple wavefront correctors. First, consider numerical simulation for a system with two wavefront correctors and two phase distorting layers. For infinite receiver aperture, if one wavefront corrector position is fixed, the dependence of the Strehl ratio $\langle St \rangle$ achieved after compensation from two wavefront correctors on the normalized distance $\hat{l}_c$ (position of the second wavefront corrector) are shown in Fig. 5. As can be seen in Fig. 5(a), when one wavefront corrector is fixed at a position ($\hat{l}_{c1} = 0.06$ or $0.03$) that is the conjugate plane of a phase screen ($\hat{l}_1 = 0.02$ or $\hat{l}_2 = 0.05$), it is better to place the second wavefront corrector at the conjugate plane ($\hat{l}_{c2} = 0.03$ or $0.06$) of the other phase screen [see Fig. 5(a)]. This verifies that the MCAO technique is effective in the case when aperture diffraction effects are neglected. However, when a finite receive aperture is considered and

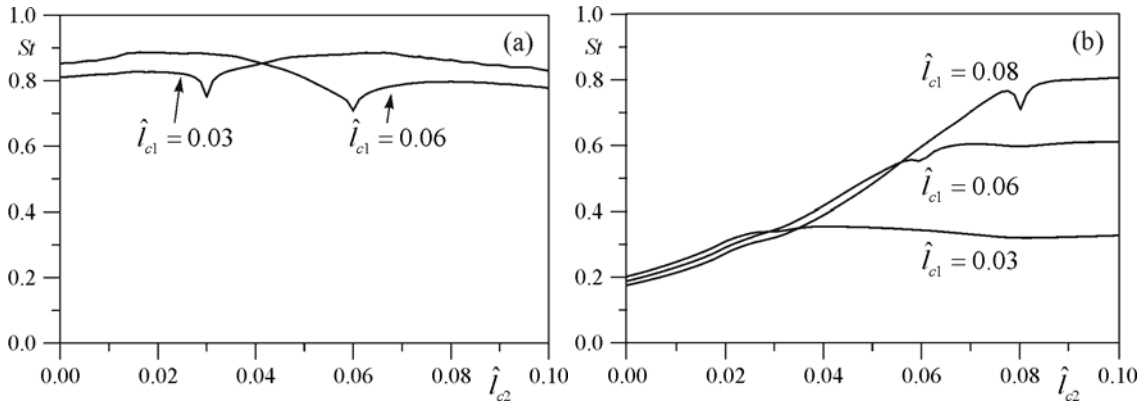


Fig. 5. Impact of the second wavefront corrector position on phase aberration compensation efficiency for two phase screens spaced at the distances $\hat{l}_1 = 0.02$ and $\hat{l}_2 = 0.05$: (a), (b) ensemble-averaged Strehl ratio versus the normalized wavefront corrector distance for high-resolution phase-conjugated control algorithms for the receiver telescope with infinite aperture (a), and for the telescope aperture coincided with the corrector aperture of size $D_c$ and $D_c = 2/3a_0$ (b). The first wavefront corrector position $\hat{l}_{c1}$ is fixed. In (a) and (b), different curves represent different first wavefront corrector positions.

one wavefront corrector is placed at the conjugate pupil plane ($\hat{l}_{c1} = 0.08$), there is no advantage of placing the second wavefront correct at either conjugate plane of the two phase screens [see Fig. 5(b)]. The best position to place the second wavefront corrector is somewhere close to the conjugate pupil plane but not exactly at this plane. In addition, adding the second wavefront corrector can only slight improve the Strehl ratio (from 0.7 to 0.8), which indicates that there is no appealing reason to add another wavefront corrector when the first wavefront corrector is placed at the conjugate pupil plane. Further, when the first wavefront corrector is placed at the conjugate plane of a phase screen ($\hat{l}_{c1} = 0.06$ or $\hat{l}_{c1} = 0.03$), no matter where the second wavefront corrector is placed, the system performance will not be improved. In fact, in this case, the compensation efficiency in terms of Strehl ratio is much worse than that obtained from placing a single wavefront corrector at the conjugate pupil plane. Again, these results verify the conclusion obtained earlier; there is no compelling reason for relocating the wavefront corrector from the conjugate plane of the telescope pupil to the conjugate planes of the phase screens.

## 5. CONCLUDING REMARKS

Propagation of optical waves over along horizontal path through continuously distributed or layered phase-distorting medium results in the development of intensity scintillations and phase singularities in the optical receiver system pupil. In this paper, both the traditional adaptive optics technique and an alternative model-free control strategy (e.g., wavefront control based on a decoupled stochastic gradient descent (D-SPGD) technique) are considered. Optimization of adaptive compensation efficiency has been carried out, which includes not only optimization of control algorithm parameters, but also identifying the optimal position for the wavefront corrector in the adaptive system wave-train. The recipe widely used in the multi-conjugate AO approach for wavefront corrector position suggests positioning the wavefront corrector in the conjugate (image) plane of the phase-distorting layer that the corrector intends to compensate. In the presented study, both receiver system aperture diffraction effects and the impact of wavefront corrector position on phase aberration compensation efficiency have been analyzed. The results show that the recipe on multi-conjugate AO approach indeed results in optimal closed-loop compensation performance, but only if aperture-induced diffraction effects can be neglected. In the presence of aperture-induced diffraction and/or for the case of multiple phase-distorting layers separated by short distances, the optimal corrector position for both closed-loop phase conjugation and D-SPGD control algorithms corresponds to the conjugate pupil-plane. Any advantage that may arise from relocation of the wavefront corrector from the plane conjugate to pupil-plane disappears in the presence of aperture diffraction effects.

Because in most cases the geometry of the phase-distorting layers location is unknown or known with some degree of uncertainty, the results presented in this paper suggest that there is no compelling reason for relocating the wavefront corrector from the conjugate plane of the telescope pupil, unless phase aberrations are the result of a

single phase-distorting layer with an accurately defined location and aperture diffraction effects neglected. In addition, aperture effects should be taken into account when evaluating the performance of an adaptive optical system. These results and analyses are expected to provide important insight for the development of high performance adaptive optic systems over long horizontal paths.

## 6. REFERENCES


1. Babcock, H.W., The possibility of compensating astronomical seeing, Publ. Astron. Soc. Pac., Vol. 65, 229-236, 1953.
2. Hardy, J.W., *Adaptive Optics for Astronomical Telescopes*, Oxford University Press, New York, 1998.
3. Roddier, F., *Adaptive Optics in Astronomy*, Cambridge University Press, New York, 1999.
4. Roggemann, M.C. and Welsh, B., *Imaging through Turbulence*, CRC Press, New York, 1998.
5. Fried, D.L. and Vaughn, J.L., Branch cuts in the phase function, Appl. Opt., Vol. 31**,** 2865-2882, 1992.
6. Fried, D.L., Branch point problem in adaptive optics, J. Opt. Soc. Am. A, Vol. 15, 2759-2768, 1998.
7. LeBigot, E.O. and Wild, W.J., Theory of branch-point detection and its implementation, J. Opt. Soc. Am. A, Vol. 16, 1724-1729, 1999.
8. Roggemann, M.C. and Koivunen, A.C., Branch-point reconstruction in laser beam projection through turbulence with finite-degree-of-freedom phase-only wave-front correction, J. Opt. Soc. Am. A, Vol. 17, 53-62, 2000.
9. Roggemann M.C. and Lee, D.J., Two-deformable-mirror concept for correcting scintillation effects in laser beam projection through the turbulent atmosphere, Appl. Opt., Vol. 37, 4577-4585, 1998.
10. Barchers, J.D., Evaluation of impact of finite-resolution effects on scintillation compensation using two deformable mirrors, J. Opt. Soc. Am. A, Vol. 18, 3098-3109, 2001.
11. Barchers, J. D., Closed-loop stable control of two deformable mirrors for compensation of amplitude and phase fluctuations, J. Opt. Soc. Am. A, Vol. 19, 926-945, 2002.
12. Becker, J.M., Detailed compensation of atmospheric seeing using multi-conjugate adaptive optics, Proc. SPIE, Vol. 1114, 215-217, 1989.
13. Ageorges, N. and Dainty, C., *Laser Guide Star Adaptive Optics for Astronomy*, Kluwer Academic Publishers, Dordrecht, Boston, London, 2000.
14. Johnston, D.C. and Welsh, B.M., Analysis of multiconjugate adaptive optics, J. Opt. Soc. Am. A, Vol. 11, 394-408, 1994.
15. Flicker, C., Sequence of phase correction in multi-conjugate adaptive optics, Opt. Lett., Vol. 26, 1743-1745, 2001.
16. Vorontsov, M.A., Justh, E.W., and Beresnev, L.A., Adaptive optics with advanced phase-contrast techniques: 1. High resolution wave-front sensing, J. Opt. Soc. Am. A, Vol. 18, 1289-1299, 2001.
17. Just, E.W. et al, Adaptive optics with advanced phase-contrast techniques: II. High-resolution wavefront control, J. Opt. Soc. Am. A, Vol. 18, 1300-1311, 2001.
18. Ellerbroek, B.L. et al, Optimizing closed-loop adaptive-optics performance with use of multiple control bandwidths, J. Opt. Soc. Am. A, Vol. 11, 2871-2886, 1994.
19. Barchers, J.D. and Ellerbroek, B.L., Improved compensation of turbulence-induced amplitude and phase distortions by means of multiple near-field phase adjustments, J. Opt. Soc. Am. A, Vol. 18, 399-411, 2001.
20. Vorontsov, M.A. and Shmalhauzen, V.I., *Principles of Adaptive Optics*, Nauka, Moscow, 1985.
21. Vorontsov, M.A., Decoupled stochastic parallel gradient descent optimization for adaptive optics: integrated approach for wave-front sensor information fusion, J. Opt. Soc. Am. A, Vol. 19, 356-368, 2002.
22. Yu, M. and Vorontsov, M.A., Compensation of distant phase-distorting layers: I. narrow field-of-view adaptive receiver, J. Opt. Soc. Am. A, Vol. 21, 1645-1658, 2004.
23. Smartt, R.N. and Steel, W.H., Theory and application of point-diffraction interferometers, Japanese Journal of Applied Physics, Vol. 14, 351-356, 1975.
24. Hariharan, P., *Selected Papers on Interferometry*, SPIE Optical Engineering Press, Bellingham, Wash., 1991.
25. Andrews, L.C., An analytic model for the refractive index power spectrum and its application to optical scintillations in the atmosphere, J. Mod. Opt., Vol. 39, 1849-1853, 1992.
26. Fried, D.L., Statistics of a geometric representation of wavefront distortion, J. Opt. Soc. Am. A, Vol. 55, 1427-1435, 1965